Stem Cell Research 32 (2018) 1–7

Contents lists available at ScienceDirect

Stem Cell Research

journal homepage: www.elsevier.com/locate/scr

Paracrine mechanisms in early differentiation of human pluripotent stem cells: Insights from a mathematical model

Erika Gaspari[a,c], Annika Franke[b], Diana Robles-Diaz[b], Robert Zweigerdt[b], Ingo Roeder[a], Thomas Zerjatke[a,**,1], Henning Kempf[b,*,1,2]

[a] Institute for Medical Informatics and Biometry, Carl Gustav Carus Faculty of Medicine, TU Dresden, Dresden, Germany
[b] Leibniz Research Laboratories for Biotechnology and Artificial Organs (LEBAO), Department of Cardiothoracic, Transplantation and Vascular Surgery (HTTG), REBIRTH-Cluster of Excellence, Hannover Medical School, Germany
[c] Laboratory of Systems and Synthetic Biology, Wageningen University & Research, Wageningen, the Netherlands

ARTICLE INFO

Keywords:
Human pluripotent stem cells
Paracrine effects
Differentiation
Primitive streak
Mathematical modeling

ABSTRACT

With their capability to self-renew and differentiate into derivatives of all three germ layers, human pluripotent stem cells (hPSCs) offer a unique model to study aspects of human development in vitro. Directed differentiation towards mesendodermal lineages is a complex process, involving transition through a primitive streak (PS)-like stage. We have recently shown PS-like patterning from hPSCs into definitive endoderm, cardiac as well as presomitic mesoderm by only modulating the bulk cell density and the concentration of the GSK3 inhibitor CHIR99021, a potent activator of the WNT pathway. The patterning process is modulated by a complex paracrine network, whose identity and mechanistic consequences are poorly understood.

To study the underlying dynamics, we here applied mathematical modeling based on ordinary differential equations. We compared time-course data of early hPSC differentiation to increasingly complex model structures with incremental numbers of paracrine factors. Model simulations suggest at least three paracrine factors being required to recapitulate the experimentally observed differentiation kinetics. Feedback mechanisms from both undifferentiated and differentiated cells turned out to be crucial. Evidence from double knock-down experiments and secreted protein enrichment allowed us to hypothesize on the identity of two of the three predicted factors. From a practical perspective, the mathematical model predicts optimal settings for directing lineage-specific differentiation. This opens new avenues for rational stem cell bioprocessing in more advanced culture systems, e.g. in perfusion-fed bioreactors enabling cell therapies.

1. Introduction

Human pluripotent stem cells (hPSCs) hold great promises for a multitude of purposes, including regenerative medicine, drug development and toxicity testing. The enormous potential of hPSCs for modern medicine is based on their capability to give rise to essentially any somatic cell type of the human body, referred to as pluripotency. To date, broad applicability of hPSC is hampered by limited robustness and understanding of the speciation processes towards a desired cell type (Denning et al., 2016; Siller et al., 2016). This is essentially due to the limited understanding of the complex regulatory networks directing the differentiation processes.

We have recently shown that even minor perturbations, i.e. simple variation in the medium volume, drastically impact on lineage-decisions in the early differentiation phase in vitro and thereby direct subsequent differentiation outcome (Kempf et al., 2016). This early differentiation phase reflects key aspects of human development during gastrulation in vivo (Arnold and Robertson, 2009). Similar to the development in vivo, upon WNT pathway stimulation, hPSCs undergo epithelial-to-mesenchymal transition and progress towards a primitive streak (PS)-like state (Skelton et al., 2016). This transition is marked by expression of the mix paired-like homeobox transcription factor 1

* Correspondence to: H. Kempf, Leibniz Research Laboratories for Biotechnology and Artificial Organs (LEBAO), Hannover Medical School, Carl-Neuberg-Str.1, 30625 Hannover, Germany.
** Correspondence to: T. Zerjatke, Institute for Medical Informatics and Biometry, Carl Gustav Carus Faculty of medicine, TU Dresden, Fetscherstr. 74, 01307 Dresden, Germany.
E-mail addresses: thomas.zerjatke@tu-dresden.de (T. Zerjatke), henningkempf@outlook.com (H. Kempf).
[1] These authors contributed equally to this work.
[2] Current address: Department of Stem Cell Biology, Novo Nordisk A/S, 2760 Maaloev, Denmark

https://doi.org/10.1016/j.scr.2018.07.025
Received 27 March 2018; Received in revised form 13 July 2018; Accepted 24 July 2018
Available online 18 August 2018

(MIXL1), which in vivo is upregulated following the invagination of cells during gastrulation (Pearce and Evans, 1999). In the course of further development, PS cells give rise to the prospective definitive endoderm and several mesodermal linages, including cardiac as well as presomitic mesoderm. These lineages form the developmental foundation of several tissues including lung, gut, heart and skeletal muscle.

By monitoring PS-like priming in the hPSC model in vitro, we have recently investigated the regulatory role of secreted proteins. Mesendodermal patterning was triggered only by the administration of CHIR99021 (Kempf et al., 2016) (a potent chemical GSK-3 inhibitor agonizing the WNT pathway (Ring et al., 2003), abbreviated in the following as CHIR) combined with variations of the bulk cell density. The study revealed that a complex interplay of stimulatory and inhibitory factors secreted by hPSC during the first 24 h of differentiation directs subsequent cell fates (Kempf et al., 2016).

To better understand the underlying mechanisms, we here complement our experimental findings with a mathematical modeling approach. This allows us to feed experimental data into mathematical simulations and, vice versa, to test the calculated predictions in our cellular model. Systems of ordinary differential equations (ODEs) have been applied to describe the first 48 h of differentiation dynamics. By adding an increasing number of regulatory feedback loops we have developed a model that is sufficiently complex to accurately describe the kinetics of the differentiation process within a broad range of experimental conditions. The model allowed us to assign specific roles to three distinct factors involved in the process. It highlights 1) the indispensability of one inhibitory factor antagonizing progression of PS priming to be released readily by undifferentiated hPSCs and 2) another inhibitory as well as one activating factor of PS progression to be upregulated and secreted at early stages of differentiation.

Moreover, we show that two secreted inhibitors of Nodal signaling, LEFTY1 and CER1, fulfill the inhibitory roles predicted by the mathematical model and also regulate expression of a MIXL1-GFP reporter used to monitor PS priming towards the expected patterns.

Finally, we are using the established model to make predictions on optimal settings for lineage-specific differentiation of perfusion-fed cells (in contrast to the typical batch-feeding used in conventional cell culture), which is relevant for advanced and automated hPSC differentiation processes.

2. Materials and methods

2.1. Experimental set-up

Differentiation was conducted on a 96-well platform applying combinations of 8 different CHIR concentrations (0–17.5 μM) and 6 medium volumes (50–300 μl) for up to 48 h using a previously established embryonic stem cell (HES-3, ESIBIe003-A) reporter line containing an eGFP in the MIXL1 locus (Davis et al., 2008) (Fig. 1A, B). For two independent replicates MIXL1 expression was determined via flowcytometry at six time points (12, 18, 24, 36 and 48 h). Experimental data of 0 μM and 2.5 μM CHIR were later excluded from the mathematical modeling as these concentrations were not sufficient for mesendodermal induction and thus represent a rather undefined population.

For validation of the mathematical model, we used a previously collected data set for mesendodermal differentiation under four different combinations of CHIR concentration and medium volume on a 12-well platform. This data set consists of six time points measured with five independent replicates. Each {CHIR/Volume} combination leads to a distinct differentiation outcome, specifically: {7.5 μM; 1 ml} to definitive endoderm, {7.5 μM; 3 ml} as well as {15 μM; 1 ml} to cardiac mesoderm and {15 μM; 3 ml} to presomitic mesoderm.

For a detailed description of experimental conditions cf. supplementary information.

2.2. Derivation of model assumptions

To develop rational assumptions for a paracrine network involved in the process, four previously reported qualitative experimental observations were considered (Kempf et al., 2016):

a) Medium refreshment experiment (Fig. 1C): The potential role of secreted factors was addressed by studying the impact of a medium change on the differentiation outcome. Refreshing the medium 6 h post induction in definitive endoderm condition (DE; 7.5 μM CHIR/50 μl, blue colour code) shifts the differentiation towards cardiac mesoderm (CM) and subsequently cardiomyogenesis (green). This accelerated PS progression upon medium refreshment consequently suggests the presence of at least one inhibitory factor in the unaltered conditions, which accumulates at an early stage and delays anteroposterior PS progression. Based on this evidence for an early release of such an inhibitory factor, we assume the factor originating from hPSCs. We refer to this factor as *X*.
b) Conditioned medium experiment (Fig. 1D): Vice versa, we studied the effect of adding enriched medium. Conditioned supernatant of the DE conditions (blue) was harvested 6 h post induction and added to the medium in presomitic mesoderm condition (PSM; 15 μM CHIR/250 μl, red). This caused a delayed differentiation progression and resulted in a shift from presomitic to cardiac mesoderm and ultimately cardiomyogenesis. Repeating the equivalent procedure by harvesting the DE supernatants after 24 h did not change the phenotype of the cells, i.e. the cells remained in the PSM condition (red). Assuming a persisting activity of the inhibitory factor X, this observation suggests the presence of at least one activatory factor, that is secreted at a later stage during PS-progression and is likely originating from MIXL1$^+$ cells. This factor is referred to as *Y*.
c) Double knock-down experiment (Fig. 1E): When two TGFβ proteins, LEFTY1 and CER1, were knocked-down by about 80%, a doubling of the fraction of MIXL1$^+$ cells was observed after 24 h (from 30% to 60%). From this observation, we hypothesized the presence of a potential second inhibitor referred to as *Z* in the mathematical model.
d) Mass spectrometry (MS) analysis of the secretome after 6 h and 24 h in DE condition: This analysis revealed that LEFTY1 is present after 6 h, while CER1 was only detected after 24 h. From these observations, we hypothesize the biological equivalent of two of the three model factors, associating X to LEFTY1 (originating from hPSCs) and Z to CER1 (originating from MIXL1$^+$ cells due to its late occurrence). No evident activatory candidates (such as growth factors from the TGFβ and WNT superfamily) as positive modulator *Y* were identified in the MS data.

In addition, the model assumptions comprise the following simplifications:

- Cell proliferation, self-renewal and apoptosis are negligible within the observed time interval (0-48 h). The total cell number is thus assumed to be constant and was experimentally determined ($\approx 8 \times 10^4$ cells/well).
- CHIR concentration and medium volume are stable over time: previous MS analysis did not show any decay of CHIR in experimental settings over 48 h (Kempf et al., 2016).
- CHIR (indirectly) inhibits the production of *X* and Z as gene expression analysis showed a ~10-fold reduction in LEFTY1 and CER1 levels at 15 μM compared to 7.5 μM CHIR independent of the medium volume (Funa et al., 2015).
- Degradation processes of *X*, *Y* and *Z* are included in the model. The degradation parameters are estimated in the model and must be interpreted as not exclusively comprising the spontaneous decay process, but a complex behavior that includes the effect of the in-vitro cultivation.

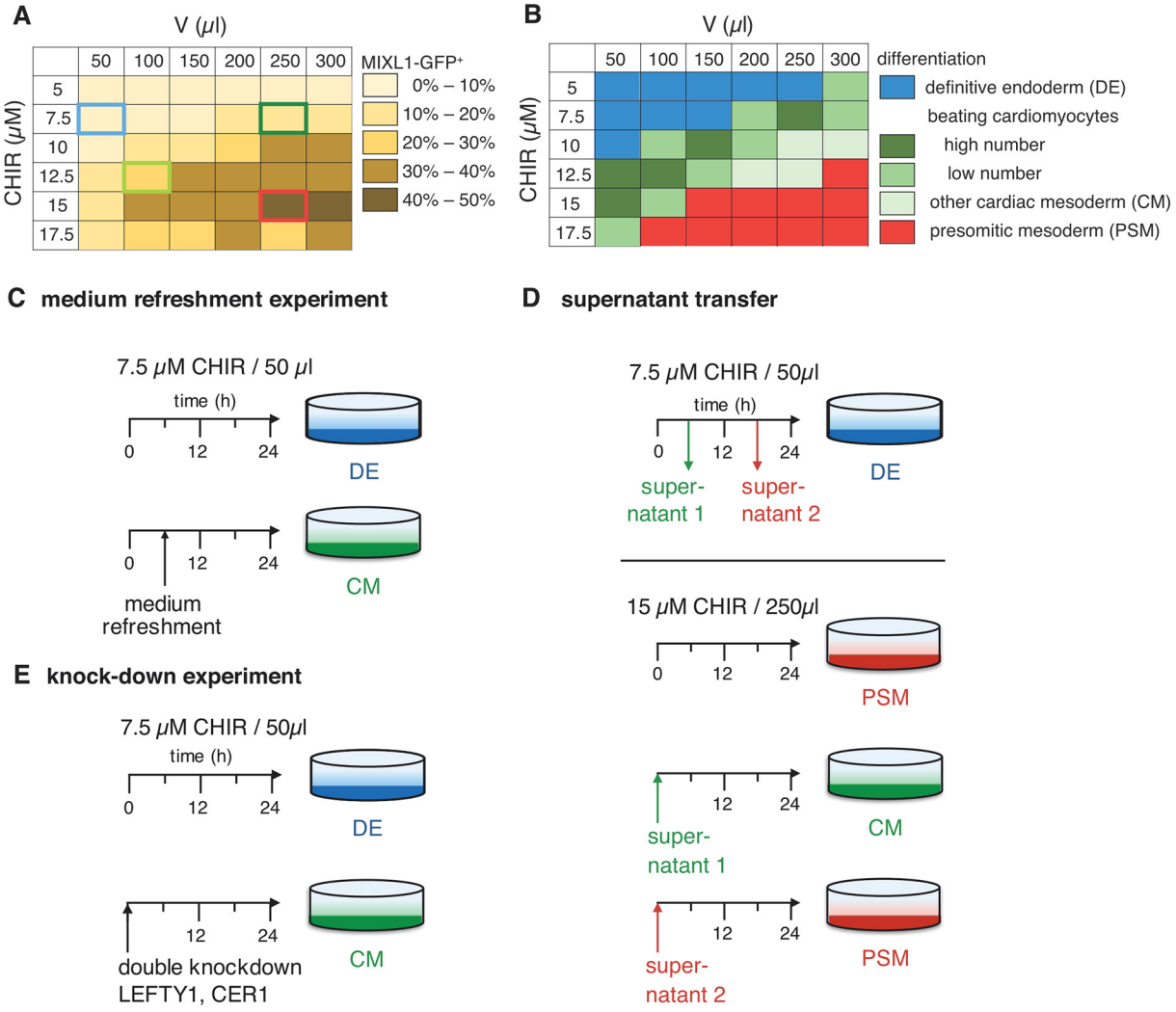

Fig. 1. (A-B) Differentiation outcome after applying indicated combinations of CHIR concentrations and medium volumes. (A) Primitive streak induction quantified by MIXL1$^+$ cells after 24 h of cultivation. Exemplary combinations of CHIR concentration and medium volumes that are shown in later figures are highlighted in colour. (B) Cell types obtained after 10 days of culture. Beating cardiomyocytes were observed in a corridor from high CHIR/low volume to low CHIR/high volume (dark green and green area). Presumptive definitive endoderm (blue) and presomitic mesoderm (red) are indicated, respectively. (C-E) Experimental observations leading to mathematical model assumptions. (C) Medium refreshment after 6 h in conditions favoring differentiation into definitive endoderm (blue, 7.5 µM CHIR, 50 µl medium volume) results in a differentiation into cardiac mesoderm (green). (D) Supernatant from definitive endoderm conditions (blue) was harvested after either 6 or 24 h. Proteins were purified and transferred into presomitic mesoderm conditions (red, 15 µM CHIR in 250 µl medium), resulting in a switch to cardiomyogenesis if the supernatant was harvested after 6 h, but not after 24 h. (E) Double knock-down of LEFTY1 and CER1 in the definitive endoderm condition shift the differentiation outcome to cardiomyogenesis and is accompanied by a two-fold increase in MIXL1$^+$. (For interpretation of the references to colour in this figure legend, the reader is referred to the web version of this article.)

2.3. Model formulation and simulation

Based on the assumptions defined above, we derive mathematical models that describe the dynamics of three cell populations: hPSCs, MIXL1$^+$, and MIXL1$^-$ cells (Fig. 2A). The latter population comprises those cells that do not undergo mesendodermal transition. Up to three regulatory paracrine factors (denoted as X, Y, and Z) are incorporated into the model. CHIR directly impacts the differentiation process, while the volume effect is indirectly reflected via cell densities and factor concentrations. The temporal behavior of cell population densities and regulatory factor concentrations is represented by ordinary differential equations (ODE).

Four different model structures (M_X, M_{XY}, M_{XZ}, and M_{XYZ}), with different complexities due to a rising number of paracrine factors, were compared to the time-course data of PS progression, indicated by MIXL1$^+$ cells.

The most complex model structure M_{XYZ} including all three paracrine factors consists of five ODEs with 14 parameters (eq. 1, for the other models cf. supplementary information). As we assume that the total number of cells and consequently the total cell density (denoted as Γ) is constant, only the dynamics of MIXL1$^+$ (denoted as M) and MIXL1$^-$ cells (denoted as N) are modeled explicitly. The density of undifferentiated hPSCs then results from the difference Γ – M – N.

Paracrine factors X, Y, and Z are produced with a certain specific production rate (denoted by p_X, p_Y, *and* p_Z, respectively) either by hPSCs (X) or MIXL1$^+$ cells (Y and Z) and are degraded by a first order kinetic with specific degradation rates, denoted by e_X, e_Y, *and* e_Z, respectively. Differentiation of hPSCs into MIXL1$^+$ cells occurs with a basal rate d_0 and is enhanced proportionally to the concentration of the activatory factor Y with rate a_y and diminished proportionally to the concentration of the inhibiting factors X and Z with rates i_x*and* i_z, resp. Differentiation into MIXL1$^-$ cells occurs unregulated with rate d_N.

Regulation by CHIR is modeled as (i) enhancing the differentiation into MIXL1$^+$ cells with rate a_C, and (ii) reducing the production of

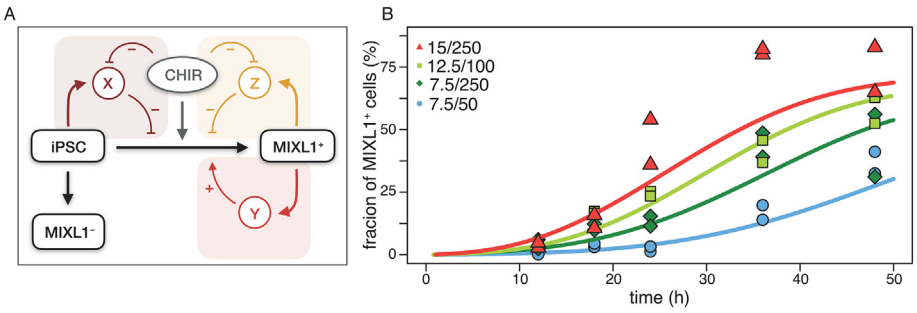

Fig. 2. (A) Mathematical model of the differentiation process. Differentiation of hPSC into MIXL1$^+$ cells is regulated by CHIR concentration and up to three paracrine factors, which either inhibit (X, Z) or enhance (Y) the process. These paracrine factors are either released by hPSCs (X) or MIXL1$^+$ cells (Y, Z). Alternatively, hPSCs can differentiate into MIXL1$^-$ cells in an unregulated manner. (B) Exemplary fits of the mathematical model including all three regulatory paracrine factors to experimental observations under four different conditions of CHIR concentration and medium volume (cf. Fig. 1A). Respective CHIR concentrations (μM) and medium volumes (μl) are indicated. Blue is representative of a presumptive condition for Definite Endoderm differentiation, green characterizes two exemplary conditions for Cardiac Mesoderm for which cardiomyogenesis was observed, red constitutes an example of Presomitic Mesoderm differentiation. (For interpretation of the references to colour in this figure legend, the reader is referred to the web version of this article.)

inhibitory factors X and Z with rates i_{CX} and i_{CZ}.

$$\mathbf{M_{XYZ}}\begin{cases}\dfrac{dM}{dt} = \dfrac{d_0 + a_C C + a_y Y}{1 + i_x X + i_z Z}(\Gamma - M - N)\\ \dfrac{dN}{dt} = d_N(\Gamma - M - N)\\ \dfrac{dX}{dt} = \dfrac{p_x}{1 + i_{cx} C}(\Gamma - M - N) - e_x X\\ \dfrac{dY}{dt} = p_y M - e_y Y\\ \dfrac{dZ}{dt} = \dfrac{p_z}{1 + i_{cz} C} M - e_z Z\end{cases} \quad (1)$$

The model output describes the evolution of the three cell population densities and the paracrine factor concentrations over time. The unknown parameters were estimated from the experimental data through a maximum likelihood estimation.

To compare the quality of the model fits, the Akaike Information Criterion (AIC) (Hu, 1987; Awad, 1996; Hu, 2007) has been computed, with the lowest AIC value representing the best fitting model structure. The goodness between model fit and validation data set has been computed by reduced chi-squared statistics (Hastings, 1970; Andrae et al., 2010). For a detailed description of the other models and on parameter estimation cf. supplementary information.

3. Results

3.1. 96 well platform of hPSC differentiation confirms patterning effects of the CHIR concentration and medium volume

Time course analysis was conducted in a 96 format by determining MIXL1 transgene expression via flow cytometry, which can be used as informative reporter of PS-like mesendoderm patterning (Kempf et al., 2016; Davis et al., 2008). The kinetics of MIXL1$^+$ levels were measured at six time points during the first 48 h of differentiation. Fig. 1A exemplarily depicts the levels for the applied CHIR-Volume matrix at 24 h post differentiation induction. The expression pattern can roughly be grouped into three different populations: 1) low MIXL1 levels indicating induction of definitive endoderm (blue condition) at low CHIR concentrations and low medium volume, 2) relative high MIXL1 levels suggesting presomitic mesoderm (red conditions) formation at high CHIR concentrations and high medium volume, and 3) induction of a presumptive 'cardiac corridor' (green conditions) spreading along high CHIR/low volume to low CHIR/high volume conditions as confirmed by beating CMs at process endpoint (dd10; Fig. 1B). These observations in the "miniaturized" 96-well format accurately reflect previous observations of the 'cardiac corridor' obtained in various experimental settings and formats including 6-, 12-, and 96-well plates (Kempf et al., 2016; Elliott et al., 2011; Rao et al., 2016).

3.2. Mathematical modeling suggests the requirement of multiple paracrine factors to recapitulate experimental data

Aiming at predicting key regulatory mechanisms controlling the differentiation process mathematical modeling was initiated. Four different models with increasing complexity were fitted to the kinetics of MIXL1 expression patterns during the first 48 h of differentiation (Fig. 2).

Model M_X comprising a single inhibitory paracrine factor *X* as well as model M_{xy} with an additional activator Y (AIC_X of 459.08; Fig. S1 and AIC_{XY} of 158.6; Fig. S2, respectively) were not sufficient to describe the experimental data for the 36 conditions displayed in Fig. 1A, B. Model M_{XYZ} including an additional inhibitory factor Z thereby resulting into five ODEs comprising 14 estimated parameters substantially improved the modeling output and was able to closely mimic the experimental data (Fig. 2B, AIC_{XYZ} of 74.28). Aiming at simplification of the model and testing the requirement of Y, we additionally optimized the parameters for model M_{XZ} (Fig. S3). However, this model completely failed to describe the data (AIC_{XZ} of 656.82).

Once verified that model M_{XYZ} is capable of describing the experimental data, the model was applied to an independent validation set of experiments (cf. suppl. Inf., Fig. S4). Importantly, for this validation step, the model parameters (Supplementary Table S1) were not refitted to the new experimental approach and the resulting data set, but applied in its original format. The resulting reduced chi-square statistics for the model validation is $\chi^2_{red} = 0.88$, implying that the model properly describes the validation experiment.

Together, this underpins the hypothesis that at least three paracrine factors are involved in the process of proper PS priming, as indicated by the MIXL1-GFP reporter.

3.3. Experimental validation of model simulations and predictions

Next, we evaluated the model's ability to predict various scenarios regarding, (1) the driving factors of differentiation, (2) single and double knock-down experiments of candidate factors, (3) optimal conditions for medium refreshment and conditioned medium experiments, and (4) the effect of perfusion feeding on the differentiation process:

3.3.1. Exploration on the driving factors of the differentiation

Model M_{XYZ} incorporates four factors shaping mesendodermal differentiation: CHIR, *X, Y, Z*. Since CHIR is known to be required for kick-starting PS-like priming of hPSC (Kempf et al., 2016), we simulated the induction of MIXL1 in the absence of CHIR (Fig. S5); the model correctly predicts the lack of induction. Furthermore, in case of the simulated absence of paracrine factors (*X, Y, Z*), the model's output behavior shows a sharp increase of MIXL1$^+$ cells (Fig. S5), attributing an important role of at least one inhibitory factor (X or Z) for shaping the differentiation process.

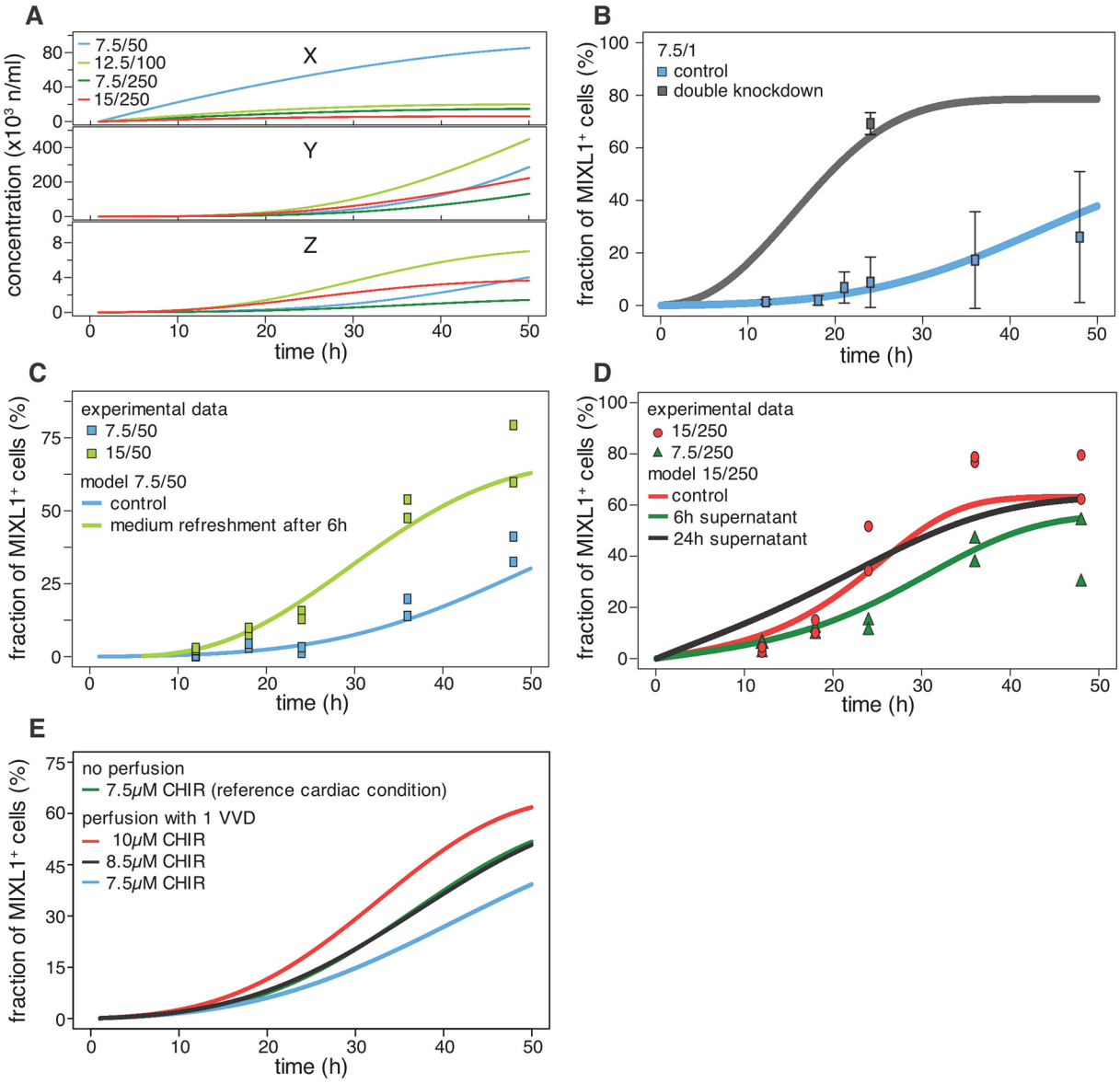

Fig. 3. (A) Concentration of the paracrine factors X, Y, Z over time resulting from model M_{XYZ} outputs for the indicated combinations of CHIR concentration (μM) and medium volumes (μl). Blue, green and red represent conditions for presumptive DE, CM and PSM, respectively. (B) Inhibitor knock-down effects on MIXL1 response for CHIR = 7.5 μM and V = 1 ml. Modeled double knock-down of X and Z reproduces the experimental observation of double knock-down of LEFTY1 and CER1 (cf. Fig. 1E), leading to an increase in MIXL1$^+$ cell density from about 10% to 60%. (C) Simulation of medium refreshment after 6 h (cf. Fig. 1C) leads to a switching from a DE (blue line) to a CM kinetic (green line). (D) Reproduction of the conditioned medium experiments (cf. Fig. 1D). Supernatant was harvested at 6 h or 24 h from DE condition and transferred into PSM medium. 6 h supernatant shifts kinetics to CM (green line), while 24 h supernatant leaves kinetics in PSM though changing its shape (black line). (E) Model predictions for continuous perfusion system. Reference cardiac condition (7.5 μM CHIR, without perfusion) is shown in green. Perfusion with a standard rate of 1 VVD (vessel volumes per day) was simulated for 7.5 μM (blue), 8.5 μM (black) or 10 μM CHIR (red). 8.5 μM CHIR closely mimics the reference kinetics. (For interpretation of the references to colour in this figure legend, the reader is referred to the web version of this article.)

Notably, the model predicts the differential temporal evolution of regulatory factors' concentrations at different experimental conditions (Fig. 3A). Interestingly, the two conditions eventually leading to cardiac mesoderm (7.5/250 and 12.5/100, green shades) show highly differential levels of paracrine factors Y and Z. This suggests that there is a high level of variability in the concentration of regulating paracrine factors in the system (likely resulting from feedback regulation loops) that can still result into the specification of the same lineage (i.e. cardiac in this example).

3.3.2. *Simulation of LEFTY1/CER1 knock-down experiments*

Applying our previous knowledge on the role of the secreted NODAL antagonist LEFTY1 and CER1 on the process (Kempf et al., 2016) (see also "derivation of model assumptions" in Material and Methods) we simulated the double knock-down of these factors. Assuming that LEFTY1 (known to be readily expressed in pluripotent hPSC) represents *X* and CER1 (known to be upregulated at early stages post CHIR treatment) represents *Z*, a calculation was performed whereby *X* and *Z* expressions was mathematically reduced by 80%. Applying the calculation to "definitive endoderm conditions" (7.5/50; blue curve in Fig. 2B) the model output of M_{XYZ} revealed a shift of MIXL1$^+$ cells from ~10% to ~60% at 24 h and predicted an overall shift of MIXL1 kinetic from "definitive endoderm" to "cardiac mesoderm" conditions, respectively (Fig. 3B). This corroborates that LEFTY1 and CER1 are the biological counterparts of the model's two inhibitory factors *X* and *Z*, respectively.

To further determine the contribution of each inhibitory factor individually, single knock-down experiments where simulated (Fig. S6). These simulations reveal varying importance of both factors depending on the chosen differentiation condition. In definitive endoderm conditions, knock-down of *Z* (CER1) did not introduce relevant changes, while knock-down of *X* (LEFTY1) showed a strong effect on the MIXL1 kinetics. In presomitic mesoderm conditions, the importance of *X* and *Z* is reverted. In cardiac mesoderm conditions, the effects of X and Z knockdowns vary depending on the chosen combination of CHIR concentration and medium volume. This again reflects the high level of plasticity in the differentiation process towards cardiac mesoderm.

3.3.3. Simulation of medium refreshment and supernatant harvesting experiments

The observations of medium refreshment experiments (see Model Assumptions and Fig. 1C) were reconstructed *in-silico* by simulating a medium exchange in the "definitive endoderm condition" after 6 h of differentiation induction. The simulation revealed that the model is capable of closely mimicking the observed biological data from respective in-vitro experiments (Fig. 3C) i.e. predicting the switch from definitive endoderm to cardiac mesoderm differentiation found in the experiment.

Additional simulations mimicking medium refreshment after 12 h, 18 h and 24 h were conducted (Fig. S7). The resulting curves intermingle between the definitive endoderm and cardiac mesoderm outcome suggesting the sensitivity of the differentiation process to precise timing of media replacement.

Conditioned medium experiments (see Model assumptions and Fig. 1D) were confirmed *in-silico* by simulating the addition of purified proteins harvested from the definitive endoderm medium after 6 h or 24 h, into PSM-oriented conditions upon differentiation start. Notably, the experimentally observed switch from presomitic to cardiac mesoderm when using 6 h harvest but not when using 24 h harvest, was indeed reflected by the mathematical modeling (Fig. 3D). Further simulation for medium replacement at 12 h and 18 h showed curve patterns more similar to medium replacement at 6 h but rather divergent compared to the exchange at 24 h (Fig. S8). This suggests that an early (< 24 h) interference with the medium volume (e.g. replacement) has a pronounced impact on the differentiation process, i.e. retards progression of PS priming towards somatic mesoderm in our model.

3.3.4. Model predictions of advanced feeding strategies by modeling a continuous perfusion system

Lastly, we applied our mathematical model to an alternative feeding strategy. In contrast to the typical "batch feeding" (entire medium replacement) applied in conventional cell culture, "continuous perfusion" settings where applied, which is of particular interest to large-scale bioprocessing in controlled bioreactors (Jara-Avaca et al., 2017; Kropp et al., 2016). Our simulations suggest, that a constant perfusion rate of 1.0 respective medium vessel volumes per day (VVD; defined by the applied process volume of the respective experimental platform) during differentiation induction at 0.33 cells/ml in 100 ml volume using a single dose of 8.5 μM CHIR without additional adjustments of the culture conditions closely mimics a reference kinetics that leads to cardiac mesoderm differentiation (7.5 μM CHIR without perfusion, Fig. 3E). Alternatively, adjusting the perfusion rate to 0.5 VVD without changing the CHIR concentration also provides a strategy to mimic the cardiac mesoderm kinetics (Fig. S9). Thus, our mathematical model predicts optimal settings for future upscaling of the differentiation process.

4. Discussion

The differentiation of hPSCs is influenced by the poorly understood interplay of secreted factors. However, in a previous study we found that the substantial regulatory impact of the bulk cell density on lineage specification is mediated by paracrine signaling (Kempf et al., 2016). Here we integrated a multitude of experimental findings into ODE models to shed light on the complex interplay of agonistic and antagonistic factors during early stages of hPSC priming and differentiation.

ODE models describe dynamic processes. Therefore, time-course analysis is required to reveal the impact of relevant parameters. To enable comprehensive multifactorial assessment over time, a previously established differentiation platform in a 12-well format (Lian et al., 2012; Kempf et al., 2014) was scaled down to 96-well plates. This strategy allowed a time course analysis over 48 h including 6 time points each comprising 6 distinct CHIR concentrations and 6 medium volumes (defining the bulk cell density), respectively. Although the overall efficiency of the MIXL1 reporter induction was somewhat lower compared to our previous 12-well format (up to 50% and up to 80% after 24 h CHIR treatment in presomitic conditions, respectively), an identical pattern of MIXL1$^+$ cell induction at early stages (Fig. 1A) and of the resulting cardiomyocyte formation (Fig. 1B) was obtained. Overall, this pattern reveals the following trends: 1) an increasing amount of MIXL1$^+$ cells is induced by an increasing medium volume (V) and increasing CHIR concentration and 2) cardiomyogenesis occurs along a vertical axis but is excluded along opposing edges i.e. at low V/low CHIR as well as high V/high CHIR, respectively (Fig. 1).

Our resulting mathematical model strongly suggest that an interplay of at least 3 paracrine factors is required to adequately recapitulate PS-like patterning; none of the more simplistic models (i.e. M_x or M_{xy}) was able to produce sufficiently accurate projections. This finding is consistent with our hypothesis that a relative complex paracrine environment is shaping early hPSC differentiation.

Based on our model in conjunction with previous MS analysis, gene expression levels and knockdown experiments (Kempf et al., 2016), LEFTY1 represents the likely candidate mediating the dominant inhibitory activity reflected by X that is released by hPSC in the early phase of differentiation. Similarly, CER1 is involved in inhibiting mesoderm formation originating from differentiation PS-like cells (Kempf et al., 2016) and consequently matches with the activity of Z. These findings are further supported by the previously described role of LEFTY1 and CER1 in restricting PS formation during mouse gastrulation (Perea-Gomez et al., 2002) and their contribution in cellular heterogeneity of hPSC culture and differentiation (Hough et al., 2014). Interestingly, our model shows a clear dependency on Y as additional activator needed to faithfully recapitulate the experimental data. Although various growth factors of the WNT/TGFβ/FGF signaling (e.g. WNT3A, WNT5A, SP5, WNT8A, BMP2, BMP4, FGF8) are transcribed during PS formation and represent potential candidates as respective biological mediators (Lian et al., 2012; Jackson et al., 2010), direct experimental evidence for distinct proteins in the microenvironment during early differentiation is essentially lacking (Kempf et al., 2016).

Several potential limitations of the modeling approach should be considered. The direct interplay and cross reaction between individual paracrine factors is neglected for simplicity. Likewise, activating and inhibitory effects are modeled in a linear fashion thus neglecting that biological, regulatory feedback loops may follow more complex kinetics (e.g. Hill kinetics). Still, this simplification is sufficient to explain the observed differentiation dynamics.

Other simplifications include our focus on distinct cell populations only (indicated as hPSCs, MIXL1$^+$ and MIXL1$^-$ cells) thus abstracting from the cellular heterogeneity of the biological system. This means that we have not accounted for the qualitative distinction of the respective cell populations, although recent research indicates qualitative differences in subpopulations at the pluripotent as well as the primitive streak state, particularly described for cells expressing differential levels of another PS marker: T-brachyury (Kempf et al., 2016; Bernardo et al., 2011; Mendjan et al., 2014). Here, for simplicity of the model, we did not attempt to discriminate between MIXL1^{low} and MIXL1^{high} cells from our flowcytometric analysis. In the future, the model might be extended to later differentiation stages including differential distinction of mesendodermal commitments by combining more lineage specific

markers. Furthermore, inclusion of additional cell lines, particularly human induced pluripotent stem cell lines, might be valuable to account for and potentially study the observed variability across hPSC lines (Toivonen et al., 2013; Nazor et al., 2012).

However, regardless of these potential shortcomings, validation of the model and additional predictions confirm our approach being sufficiently complex to describe key steps of mesendodermal development in vitro.

Mathematical modeling has been broadly applied to help understanding self-maintenance and differentiation of stem cells, e.g. for hematopoietic stem cells (Mackey, 2001; Wilson et al., 2008; Marciniak-Czochra et al., 2009; Glauche et al., 2007) or ES cells (Herberg et al., 2015). However, the mathematical model presented here is among the first to describe mesendodermal differentiation of hPSCs. Interestingly, Tewary et al. recently used a reaction-diffusion model to describe self-regulated patterning of hPSCs (Tewary et al., 2017). While the authors primarily address the spatial organization in defined, surface attached hPSC colonies (2D), our present study focuses on the global paracrine environment driving mesendodermal patterning, which in principle applies to all culture formats including 3D suspension culture. Thus, the approaches are complementary and both help to understand the complexity of the differentiation process.

In conclusion, we have established a mathematical model that cannot only accurately describe key aspects of the differentiation process towards mesendoderm but also predicts differentiation outcomes under modified culture conditions. This is particularly necessary regarding more advanced bioprocessing setups, such as perfusion system in stirred tank bioreactors (Kropp et al., 2016).

Acknowledgment

We thank Hans H. Diebner and Walter de Back for advice in parameter estimation. This work was funded by TECHNOBEAT (European Union H2020 grant 668724), the add-on fellowship for interdisciplinary science by the Joachim Herz Stiftung (to H.K.), as well as MHH Hannover (HiLF grant to H.K.). The collaboration was facilitated by the German Stem Cell Network (GSCN). We acknowledge support by the Open Access Publication Funds of the SLUB/TU Dresden.

Appendix A. Supplementary data

Supplementary data to this article can be found online at https://doi.org/10.1016/j.scr.2018.07.025.

References

Andrae, R., Schulze-Hartung, T., Melchior, P., 2010. Dos and Don'ts of Reduced Chi-Squared. arXiv preprint arXiv:1012.3754. .
Arnold, S.J., Robertson, E.J., 2009. Making a commitment: cell lineage allocation and axis patterning in the early mouse embryo. Nat. Rev. Mol. Cell Biol. 10, 91–103.
Awad, A.M., 1996. Properties of the Akaike information criterion. Microelectron. Reliab. 36, 457–464.
Bernardo, A.S., Faial, T., Gardner, L., Niakan, K.K., Ortmann, D., Senner, C.E., Callery, E.M., Trotter, M.W., Hemberger, M., Smith, J.C., Bardwell, L., Moffett, A., Pedersen, R.A., 2011. BRACHYURY and CDX2 mediate BMP-induced differentiation of human and mouse pluripotent stem cells into embryonic and extraembryonic lineages. Cell Stem Cell 9, 144–155.
Davis, R.P., Ng, E.S., Costa, M., Mossman, A.K., Sourris, K., Elefanty, A.G., Stanley, E.G., 2008. Targeting a GFP reporter gene to the MIXL1 locus of human embryonic stem cells identifies human primitive streak-like cells and enables isolation of primitive hematopoietic precursors. Blood 111, 1876–1884.
Denning, C., Borgdorff, V., Crutchley, J., Firth, K.S., George, V., Kalra, S., Kondrashov, A., Hoang, M.D., Mosqueira, D., Patel, A., Prodanov, L., Rajamohan, D., Skarnes, W.C., Smith, J.G., Young, L.E., 2016. Cardiomyocytes from human pluripotent stem cells: from laboratory curiosity to industrial biomedical platform. Biochim. Biophys. Acta 1863 (, 1728–1748.
Elliott, D.A., Braam, S.R., Koutsis, K., Ng, E.S., Jenny, R., Lagerqvist, E.L., Biben, C., Hatzistavrou, T., Hirst, C.E., Yu, Q.C., Skelton, R.J., Ward-Van Oostwaard, D., Lim, S.M., Khammy, O., Li, X., Hawes, S.M., Davis, R.P., Goulburn, A.L., Passier, R., Prall, O.W., Haynes, J.M., Pouton, C.W., Kaye, D.M., Mummery, C.L., Elefanty, A.G., Stanley, E.G., 2011. NKX2-5(eGFP/w) hESCs for isolation of human cardiac progenitors and cardiomyocytes. Nat. Methods 8, 1037–1040.
Funa, N.S., Schachter, K.A., Lerdrup, M., Ekberg, J., Hess, K., Dietrich, N., Honore, C., Hansen, K., Semb, H., 2015. Beta-Catenin Regulates Primitive Streak Induction through Collaborative Interactions with SMAD2/SMAD3 and OCT4. Cell Stem Cell 16, 639–652.
Glauche, I., Cross, M., Loeffler, M., Roeder, I., 2007. Lineage specification of hematopoietic stem cells: mathematical modeling and biological implications. Stem Cells 25, 1791–1799.
Hastings, N.A.J., 1970. The Chi-squared distribution. J. Oper. Res. Soc. 21, 383–384.
Herberg, M., Zerjatke, T., de Back, W., Glauche, I., Roeder, I., 2015. Image-based quantification and mathematical modeling of spatial heterogeneity in ESC colonies. Cytometry A 87, 481–490.
Hough, S.R., Thornton, M., Mason, E., Mar, J.C., Wells, C.A., Pera, M.F., 2014. Single-cell gene expression profiles define self-renewing, pluripotent, and lineage primed states of human pluripotent stem cells. Stem Cell Rep. 2, 881–895.
Hu, S., 1987. Book review: Akaike information criterion statistics. Math. Comput. Simul. 29, 452.
Hu, S., 2007. Akaike information criterion. Cent. Res, Sci. Comput. http://www4.ncsu.edu/~shu3/Presentation/AIC_2012.pdf.
Jackson, S.A., Schiesser, J., Stanley, E.G., Elefanty, A.G., 2010. Differentiating embryonic stem cells pass through 'temporal windows' that mark responsiveness to exogenous and paracrine mesendoderm inducing signals. PLoS One 5, e10706.
Jara-Avaca, M., Kempf, H., Ruckert, M., Robles-Diaz, D., Franke, A., de la Roche, J., Fischer, M., Malan, D., Sasse, P., Solodenko, W., Drager, G., Kirschning, A., Martin, U., Zweigerdt, R., 2017. EBIO does not induce cardiomyogenesis in human pluripotent stem cells but modulates cardiac subtype enrichment by lineage-selective survival. Stem Cell Rep. 8, 305–317.
Kempf, H., Olmer, R., Kropp, C., Ruckert, M., Jara-Avaca, M., Robles-Diaz, D., Franke, A., Elliott, D.A., Wojciechowski, D., Fischer, M., Roa Lara, A., Kensah, G., Gruh, I., Haverich, A., Martin, U., Zweigerdt, R., 2014. Controlling expansion and cardiomyogenic differentiation of human pluripotent stem cells in scalable suspension culture. Stem Cell Rep. 3, 1132–1146.
Kempf, H., Olmer, R., Haase, A., Franke, A., Bolesani, E., Schwanke, K., Robles-Diaz, D., Coffee, M., Gohring, G., Drager, G., Potz, O., Joos, T., Martinez-Hackert, E., Haverich, A., Buettner, F.F., Martin, U., Zweigerdt, R., 2016. Bulk cell density and Wnt/TGFbeta signalling regulate mesendodermal patterning of human pluripotent stem cells. Nat. Commun. 7, 13602.
Kropp, C., Kempf, H., Halloin, C., Robles-Diaz, D., Franke, A., Scheper, T., Kinast, K., Knorpp, T., Joos, T.O., Haverich, A., Martin, U., Zweigerdt, R., Olmer, R., 2016. Impact of feeding strategies on the scalable expansion of human pluripotent stem cells in single-use stirred tank bioreactors. Stem Cells Transl. Med. 5, 1289–1301.
Lian, X., Hsiao, C., Wilson, G., Zhu, K., Hazeltine, L.B., Azarin, S.M., Raval, K.K., Zhang, J., Kamp, T.J., Palecek, S.P., 2012. Robust cardiomyocyte differentiation from human pluripotent stem cells via temporal modulation of canonical Wnt signaling. Proc. Natl. Acad. Sci. U. S. A. 109, E1848–E1857.
Mackey, M.C., 2001. Cell kinetic status of haematopoietic stem cells. Cell Prolif. 34, 71–83.
Marciniak-Czochra, A., Stiehl, T., Ho, A.D., Jäger, W., Wagner, W., 2009. Modeling of asymmetric cell division in hematopoietic stem cells—regulation of self-renewal is essential for efficient repopulation. Stem Cells Dev. 18, 377–386.
Mendjan, S., Mascetti, V.L., Ortmann, D., Ortiz, M., Karjosukarso, D.W., Ng, Y., Moreau, T., Pedersen, R.A., 2014. NANOG and CDX2 pattern distinct subtypes of human mesoderm during exit from pluripotency. Cell Stem Cell 15, 310–325.
Nazor, K.L., Altun, G., Lynch, C., Tran, H., Harness, J.V., Slavin, I., Garitaonandia, I., Muller, F.J., Wang, Y.C., Boscolo, F.S., Fakunle, E., Dumevska, B., Lee, S., Park, H.S., Olee, T., D'Lima, D.D., Semechkin, R., Parast, M.M., Galat, V., Laslett, A.L., Schmidt, U., Keirstead, H.S., Loring, J.F., Laurent, L.C., 2012. Recurrent variations in DNA methylation in human pluripotent stem cells and their differentiated derivatives. Cell Stem Cell 10, 620–634.
Pearce, J.J., Evans, M.J., 1999. Mml, a mouse Mix-like gene expressed in the primitive streak. Mech. Dev. 87, 189–192.
Perea-Gomez, A., Vella, F.D., Shawlot, W., Oulad-Abdelghani, M., Chazaud, C., Meno, C., Pfister, V., Chen, L., Robertson, E., Hamada, H., Behringer, R.R., Ang, S.L., 2002. Nodal antagonists in the anterior visceral endoderm prevent the formation of multiple primitive streaks. Dev. Cell 3, 745–756.
Rao, J., Pfeiffer, M.J., Frank, S., Adachi, K., Piccini, I., Quaranta, R., Arauzo-Bravo, M., Schwarz, J., Schade, D., Leidel, S., Scholer, H.R., Seebohm, G., Greber, B., 2016. Stepwise Clearance of Repressive Roadblocks Drives Cardiac Induction in Human ESCs. Cell Stem Cell 18, 341–353.
Ring, D.B., Johnson, K.W., Henriksen, E.J., Nuss, J.M., Goff, D., Kinnick, T.R., Ma, S.T., Reeder, J.W., Samuels, I., Slabiak, T., Wagman, A.S., Hammond, M.E., Harrison, S.D., 2003. Selective glycogen synthase kinase 3 inhibitors potentiate insulin activation of glucose transport and utilization in vitro and in vivo. Diabetes 52, 588–595.
Siller, R., Naumovska, E., Mathapati, S., Lycke, M., Greenhough, S., Sullivan, G.J., 2016. Development of a rapid screen for the endodermal differentiation potential of human pluripotent stem cell lines. Sci. Rep. 6, 37178.
Skelton, R.J., Brady, B., Khoja, S., Sahoo, D., Engel, J., Arasaratnam, D., Saleh, K.K., Abilez, O.J., Zhao, P., Stanley, E.G., Elefanty, A.G., Kwon, M., Elliott, D.A., Ardehali, R., 2016. CD13 and ROR2 Permit Isolation of Highly Enriched Cardiac Mesoderm from Differentiating Human Embryonic Stem Cells. Stem Cell Rep. 6, 95–108.
Tewary, M., Ostblom, J., Prochazka, L., Zulueta-Coarasa, T., Shakiba, N., Fernandez-Gonzalez, R., Zandstra, P.W., 2017. A stepwise model of reaction-diffusion and positional information governs self-organized human peri-gastrulation-like patterning. Development 144, 4298–4312.
Toivonen, S., Ojala, M., Hyysalo, A., Ilmarinen, T., Rajala, K., Pekkanen-Mattila, M., Aanismaa, R., Lundin, K., Palgi, J., Weltner, J., Trokovic, R., Silvennoinen, O., Skottman, H., Narkilahti, S., Aalto-Setala, K., Otonkoski, T., 2013. Comparative analysis of targeted differentiation of human induced pluripotent stem cells (hiPSCs) and human embryonic stem cells reveals variability associated with incomplete transgene silencing in retrovirally derived hiPSC lines. Stem Cells Transl. Med. 2, 83–93.
Wilson, A., Laurenti, E., Oser, G., van der Wath, R.C., Blanco-Bose, W., Jaworski, M., Offner, S., Dunant, C.F., Eshkind, L., Bockamp, E., 2008. Hematopoietic stem cells reversibly switch from dormancy to self-renewal during homeostasis and repair. Cell 135, 1118–1129.